



# Velocity and concentration distribution in slurry pipe flow

O.A. El Masry, M.M. El Halawany

*Mechanical Engineering Department, Faculty of Engineering, Alexandria University, Alexandria 21544, Egypt*

## ABSTRACT

This paper presents theoretical analysis and experimental verification of the velocity and concentration fields in a low concentration steady slurry turbulent flow in a horizontal pipe. The velocity distribution was obtained by the integration of the linear momentum equation. The velocity gradient was considered as the result of the gravitational force, hindered turbulent motion, concentration distribution of the solid particles and mixing effects due to the interaction of the liquid and the solid particles. The obtained explicit algorithm does not require system of equations to be solved. An experiment was designed and carried out to test the theoretical model. Using sand-water suspension of up to 10% solid concentration and an average velocity of up to 2.4 m/s in a 18.35 m length and 33 mm I.D. pipeline. Concentration distribution was measured using gamma-ray absorption principle. Velocity profiles were measured using Pitot-tube system. The results of the experiment showed that the theoretical model is able to reflect particle and fluid property effects on the prediction of the flow velocity distribution for low volumetric concentration of steady slurry flow.

## NOTATIONS

a	experimental coefficient in Eqn. (21)	s	subscript for solid phase
$C_d$	drag coefficient	U	flow velocity, (m/s)
c	concentration volume fraction %	v <sub>r</sub>	friction velocity, (m/s)
$c_b$	bottom concentration at (0.03D) %	v <sub>s</sub>	settling velocity, (m/s)
$c_p$	packing concentration %	x,y,z	cartesian coordinates
d	particle diameter, (m)	Y	translated vertical coordinate
D	pipe diameter, (m)		
e	kinematic diffusion coefficient, (m)		<i>Greek Letters</i>
f	friction factor	$\alpha$	turbulence coefficient
h	pipe roughness, (m)	$\beta$	coefficient of relative velocity
K	variable defined by Eqns. (8) & (9)	$\mu$	dynamic viscosity, (N.s/m <sup>2</sup> )
l	subscript for liquid phase	$\nu$	kinematic viscosity, (m <sup>2</sup> /s)



## 84 Computational Methods and Experimental Measurements

L	tube length, (m)	$\rho$	density, (kg/m <sup>3</sup> )
m	subscript for mixture	$\tau$	shear stress, (N/m <sup>2</sup> )
n	experimental coefficient in Eqn. (14)		
p	pressure, (Pa)	<u>Non-Dimensional numbers</u>	
R	interaction force per unit volume, (N/m <sup>3</sup> )	Fr	modified Froude number [(v. <sup>3</sup> )/(gd(S-1))]
r	radial distance in the tube, (m)	Re	Reynolds number [(UD)/ $\nu$ ]
S	specific gravity ratio = ( $\rho/\rho_1$ )		

### INTRODUCTION

Attempts to deal with slurry flow problems may be divided into two main categories. In the first approach, one begins from experimental facts and generalizes known correlations for some parameter by dimensional analysis, without providing an insight into the flow structure, Duarand [1], Condolios [2], Zandi and Govatos [3] and Baird et al [4]. In the second approach, one starts from the momentum equations for two phase flow and numerically solves them for specific conditions utilizing physical or mathematical assumptions for different terms Bagnold [5], Wilson [6] and Roco and Shook [7] & [8]. The later approach explains many of the experimental findings related to interaction through contact between solid particles in the flow or between particle and the pipe wall.

Because of complexity of the two-phase flow systems, a complete description of the flow based only on differential equations is not possible. The model must contain some intuitive or empirical components.

The majority of the previous analytical treatments of the turbulent motion of liquid-solid mixtures have modified the momentum transfer approach of homogeneous flow. Concepts such as mixing length, Yalin [9], von Karman constant variation, Warg [10] or diffusion coefficient, Shook and Daniel [11] were employed. The presence of solid particles was considered to increase the degree of turbulence in all these studies. Computational results of these models have been applied to only a limited quantity of experiments.

The present paper suggests a new hypothesis in the study of turbulent slurry flow by integration of the governing equations using rational assumptions and experimental measurements for the concentration distribution to calculate the velocity profiles in the pipeline.

### ANALYSIS

For homogeneous flow of suspension of solid particles defined by their diameter and moving with pure translational motion, the steady one-dimensional Cauchy momentum equations in a horizontal pipe are:

$$0 = - (1-c) \frac{dP}{dz} + \frac{\partial(\tau_l)_{zx}}{\partial x} + \frac{\partial(\tau_l)_{zy}}{\partial y} + (R_l)_z \quad (1)$$

$$0 = - c \frac{dP}{dz} + \frac{\partial(\tau_s)_{zy}}{\partial x} + \frac{\partial(\tau_s)_{yz}}{\partial y} + (R_s)_z \quad (2)$$

The specific interaction forces per unit volume between two phases are equal in magnitude and of opposite sense i.e :

$$(R_l)_z = - (R_s)_z \quad (3)$$

## Computational Methods and Experimental Measurements 85

Summing equations (1) and (2) and using equation (3), we obtain :

$$0 = -\frac{dP}{dz} + \frac{\partial(\tau_m)_{zx}}{\partial x} + \frac{\partial(\tau_m)_{zy}}{\partial y} \quad (4)$$

where  $(\tau_m)_{zx} = (\tau_v)_{zx} + (\tau_t)_{zx}$  (5)

and  $(\tau_m)_{zy} = (\tau_v)_{zy} + (\tau_t)_{zy}$

The shear stress  $\tau_m$  is considered to contain two terms, one due to the friction between two neighboring layers of different velocity (viscous component) and another due to the turbulent exchange of mass between these layers.

$$(\tau_m)_{zx} = \mu_m \frac{\partial U_m}{\partial x} + \frac{\partial(\rho_m \alpha_m U_m^2)}{\partial x} \quad (6)$$

i.e.

$$(\tau_m)_{zy} = \mu_m \frac{\partial U_m}{\partial y} + \frac{\partial(\rho_m \alpha_m U_m^2)}{\partial y}$$

$U_m$  is the average mixture velocity and  $\rho_m$ ,  $\mu_m$  and  $\alpha_m$  are the mixture density, viscosity and turbulent coefficient respectively.

Substituting of equation (6) into equation (4) and neglecting the second order effect of the viscosity:

$$\frac{dP}{dz} = \frac{d^2}{dx^2} (\mu_m U_m + \rho_m \alpha_m U_m^2) + \frac{d^2}{dy^2} (\mu_m U_m + \rho_m \alpha_m U_m^2) \quad (7)$$

or  $dP/dz = \nabla^2 K$  (8)

where  $K = \mu_m U_m + \rho_m \alpha_m U_m^2$  (9)

Equation (9) is a quadratic equation in  $U_m$  and is solved directly to give:

$$U_m = U_m(y) = \frac{-\mu_m}{2\rho_m \alpha_m} + \sqrt{\frac{\mu_m}{4\rho_m^2 \alpha_m^2} + \frac{K}{\rho_m \alpha_m}} \quad (10)$$

where the term  $K$  is a function of  $U_m$  and hence of  $y$ .  $K$  is obtained from equation (8) and the boundary conditions

$$K(y) \quad \text{at } y = D/2$$

$$\frac{\partial K(y)}{\partial y} = 0 \quad \text{at } y = 0 \quad (11)$$

The above simplified symmetric velocity profile is used since the expected profile deviates from the symmetric shape only at the bottom of the tube.  $K$  may then be obtained as:

$$K(y) = -\frac{1}{2} \left( \frac{dP}{dz} \right) \left( \frac{D^2}{4} - y^2 \right) \quad (12)$$

The coordinate  $y$  is translated to the bottom of the tube i.e.

$$K(Y) = -\left( \frac{dP}{dz} \right) \frac{Y}{2} (D-Y) \quad (13)$$



## 86 Computational Methods and Experimental Measurements

Equation (10) gives the mixture axial velocity distribution in the vertical mid-plane of the tube cross-section at length  $z$ . Coefficients  $\mu_m$ ,  $\rho_m$  and  $\alpha_m$  are functions of the concentration distribution  $c(Y)$  and are obtained as follows:

### Kinematic viscosity of the mixture $\mu_m$

Volcaldo and Charles [12] estimated the kinematic viscosity of a mixture  $\mu_m$  using the expression

$$\mu_m = \mu_l \frac{\exp(2.5c - nc/c_p)}{(1 - c/c_p)} \quad (14)$$

where

$c_p$  is the packing concentration, and  
 $n$  is an experimental coefficient ( $n = 2$  for sand)

### Density of the mixture $\rho_m$

The mixture apparent density is a function of the densities of both the liquid and solid components and the local concentration as given by Wallis [13]:

$$\rho_m = (1 - c) \rho_l + c \rho_s \quad (15)$$

### Turbulence coefficient $\alpha_m$

It is defined to have two components reflecting the presence of the two phases [7]:

$$\alpha_m = (1 - c) \frac{\rho_l}{\rho_s} \times \alpha_l(s) + c \frac{\rho_s}{\rho_m} \times \beta \times \alpha_s \quad (16)$$

where  $\beta$  is a relative velocity coefficient and is considered equals unity for low concentration.  $\alpha_l$ , the turbulent coefficient for liquid flowing in a circular pipe has a semiempirical expression [12] valid for any position  $Y$  and any surface roughness  $h$ ,

$$\alpha_l = Y \left(1 - \frac{Y}{D}\right) \left[ 8.5 + 5.75 \log_{10} \frac{Y}{h + 3.3v/v_*} \right]^2 \quad (17)$$

where  $v_*$ , the turbulent velocity calculated from the experimental pressure drop per unit length  $(\Delta p)/L$ :

$$v_* = \sqrt{\frac{\tau_w}{\rho}} \text{ and } \tau_w = \frac{D}{4} \left( \frac{\Delta P}{L} \right) \quad (18)$$

the incremental change in the mixture turbulent coefficient  $\alpha_m$  is related to  $\alpha_l$  as

$$\frac{\Delta \alpha_m}{\Delta \alpha_l} = (1 - c) \frac{\rho_l}{\rho_m} \frac{\Delta \alpha_l(s)}{\Delta \alpha_l} + c \frac{\rho_s}{\rho_m} \frac{\Delta \alpha_s}{\Delta \alpha_l} \quad (19)$$

where  $\alpha_l(s)$  is the turbulent coefficient of the liquid due to the presence of the solid particles defined by:

$$\frac{\Delta \alpha_l(s)}{\Delta \alpha_l} = 1 - \frac{c}{c_p} \quad (20)$$

The turbulent coefficient  $\alpha_s$ , due to the solid particle concentration in the mixture is defined



as:

$$\frac{\Delta a_s}{\Delta a_l} = \frac{1}{\left(1 - \frac{c}{c_p}\right)^a \left(1 - \frac{1}{Fr}\right)} \quad (21)$$

where  $a$  is an experimental coefficient taken as 1.8 and  $Fr = V^2 / gd(S-1)$  is the modified Froude number [7] representing the sedimentation tendency.

### Concentration Distribution

It is required to know the distribution of the particle concentration in the mid vertical plane of the pipe to perform the calculation of the velocity distribution given by equation (10). The concentration distribution was measured using gamma-ray technique as will be given in the experimental section. These measurements were correlated using a formula proposed by Roco and Frasinéanu [16] in which initial value of concentration  $c_b$  was imposed at  $Y = 0.03 D$ :

$$C(Y) = \frac{C_b}{\frac{c_b}{c_p} + \left(1 - \frac{c_b}{c_p}\right) \times \exp\left(-\frac{v_s Y}{e}\right)} \quad (22)$$

where  $e$  the average kinematic diffusion coefficient defined in [16] and is proportional to  $(1 - c/c_p)$

## EXPERIMENTAL WORK

### Apparatus

The model has been tested with data obtained in a closed loop laboratory system, using galvanized steel pipes of 33 mm inside diameter and Prespex test section of the same diameter, the total length of the pipeline was 18.35 m with the transparent test section of 1.84 m. The pipeline was equipped with a mixing tank, a centrifugal pump of 1.5 kW power and a number of controlling valves. The mixing tank served the purpose of mixing the suspension to keep the concentration at its pre-set value. A schematic diagram of the flow system is given in figure (1). Details of the system could be found elsewhere [17].

The pressure gradient was obtained through measurements of the pressure drop across the test section using a calibrated differential pressure transducer (CELSECO, Model KP 15) with an accuracy of  $\pm 2$  Pa, and read-out unit (CELESCO, Model CD25C).

Measurements of the slurry steady flow rate were obtained through a calibrated Venturi meter and a differential pressure transducer (CELSCO, Model XP30) with accuracy of  $\pm 10$  Pa. Flow rate and pressure gradient measurements were used to obtain the friction factor Reynolds number relationship for the pure water flowing in the system:

$$f = 0.118 Re^{-0.158} \quad (23)$$

The slurry suspension used was a mixture of sand-water. The sand, locally available, was of one mesh size of 25 and a particle average diameter of 0.91 mm. Other properties with their accuracy were as follows:

Particle specific weight	$2.65 \pm 0.03 \text{ gm/cm}^3$
Particle settling velocity ( $v_s$ )	$12.30 \pm 0.20 \text{ cm/s}$
Average drag coefficient $C_D$	$1.31 \pm 0.04$



## 88 Computational Methods and Experimental Measurements

Maximum packing concentration  $c_p$  0.58

### Concentration Distribution Measurements

Gamma - ray absorption technique was employed in measurements of chord-average concentration. The technique is one of the most accurate and simple techniques. It consists of a gamma-ray source (CS 137) and a matched scintillation counter detector. The source and detector were mounted on a horizontal bar traversing in the vertical direction on a graduated scale. The source and detector were aligned optically on the bar which was leveled in the horizontal plane across the tube. The vertical motion of the bar allowed scanning of the tube cross section. The mechanism is shown in figure (2).

Positions of measurements are given in figure (3). Calibration of the system was achieved in position with pure water flowing in the pipeline. Absorption coefficients for sand-water were established in static calibration. A check on the concentration distribution was obtained by the integration over the cross-section and comparison with the average concentration value. Maximum deviation of 7% indicated accurate measurements of concentration

### Velocity Distribution Measurements

Pitot tube system is simple, inexpensive and, in skilled hands, can give extremely accurate results. The system is proposed to correct mean velocity measurements with more advanced techniques, Kassab [18] such as hot- wire probes and laser doppler anemometry (LDA).

The pitot-tube system used for measurements of the mean velocity distribution consisted of a transverse tube made of a stainless steel needle (2mm) with a side hole (0.5 mm) drilled near the blocked end. The tube moved across the tube through a sealed guide. Opposite to the needle a lateral hole for static pressure measurements was made. Figure (4) gives details of the tube design. The two terminals of the Pitot system were connected to the two sides of a calibrated differential pressure transducer (CELESCO Model KP 15) and the output was fed to the reading unit and displayed on a digital voltmeter. Accuracy of the transducer was obtained to be  $\pm 1\text{Pa}$ .

The measurements of the velocity profile were undertaken in both the vertical and horizontal planes by rotation of the pipe collars holding the Pitot system for  $90^\circ$ . Positioning of the Pitot tube inside the tube was

achieved using a vernier caliber traversing in steps of 1 mm. Measurement positions across the pipe are given in Figure (5). Readings were taken across the pipe section as the tube traversed forward and backward. Average of the two readings at each location was taken as a measure of the velocity.

Calibration of the Pitot tube system was obtained for a fully developed turbulent flow of water in the pipeline using Prandtl's formula for a rough pipe, Yuan [19]:

$$\frac{U_{\max} - U}{v_*} = \frac{1}{0.23} \left[ \ln \left( \frac{1 + \sqrt{2r/D}}{1 - \sqrt{2r/D}} \right) - 2 \sqrt{\frac{2r}{D}} \right] \quad (24)$$

where  $v_*$  is the friction velocity, is defined by equation (8) and was calculated from pressure gradient measurements. Figure (6) gives the calibration curve indicating a maximum deviation of 5%.



## RESULTS AND DISCUSSION

Testing of the velocity distribution using the proposed model given by Equation (10) requires, in addition to the velocity measurements, the measurements of both the concentration distribution in the vertical mid-plane and the pressure gradient. Experiments covering volumetric concentration ( $c$ ) range of approximately 3-10% with average flow velocity ( $u$ ) of the range (1.16-2.35 m/s), were carried out. Table 1 gives details of the performed experiments.

Concentration distribution measurements are given in Figures (7-9). In general the concentration of the solid particles was high near the bottom of the tube and decreased gradually to leave pure water near the top of the tube. Increasing average velocity of the flow, the slurry regime approached the homogeneous state with a noticeable redistribution of the particles from the bottom upwardly. This is shown in figure (7) where the slurry concentration was held at 3% and the flow average velocity increased from 1.16 to 1.95 m/s.

To compare our measurements with the available model for concentration distribution proposed by Roco and Fransieneanu [16] and given by Eq. (22), value of the bottom concentration was extrapolated from the measurements. Maximum packing concentration was taken as 0.58 as given in [16] and the average kinematic diffusion coefficient was calculated for each experiment. Figure (8) gives comparison between our measurements for concentration of 5% at different flow rates and the prediction given by the Roco & Fransieneanu model [16]. The model agreed well with the measurements, however, at low values the deviation was considerably high.

Comparison of the concentration profiles for the same mean flow velocity ( $U = 2.35$  m/s) and different volumetric concentration (3,5 and 7%) is given in Figure (9). The profile for 3% concentration showed near heterogeneous flow regime while increasing the concentration allowed the solid particles to settle towards the bottom and changed the slope of the profile to a steeper one with higher concentration at the lower half of the pipe. Roco & Fransieneanu model [16] underestimated the measurements at low concentration (3%) while overestimated them at higher concentration (7, 10%). This is due to the fact that the model main parameter is the bottom concentration while the particle size, shape and properties are not taken into consideration .

Velocity distribution at both the vertical and horizontal mid-planes were measured. In the horizontal plane, the velocity distribution showed very near symmetric profile at all the performed experiments. A result which was expected from flow in a circular symmetric pipeline. In the vertical mid-plane, the velocity distribution, figures (10) and (11), was asymmetric with the dynamic (D.A.) appeared above the geometric axis. This was due to asymmetric distribution of the solid particles across the tube. At the upper half of the tube the flow was more faster than that at the lower half since it carried less solids. Figures (10) and (11) showed the comparison between the experimental measurements of the velocity distribution in the vertical mid-plane and the data calculated using the present proposed model given by equation (10). In all our experiments, the experimental measurements of the velocity and the calculated profiles showed good agreement with maximum deviation of 7% indicating accurate model prediction of the velocity . Figure (10) shows the change in the velocity profile,



## 90 Computational Methods and Experimental Measurements

as the average flow velocity was increased while keeping the average concentration the same. Increasing the flow velocity forced the dynamic axis of the profile closer to the geometric axis and brought the distribution to the near symmetric shape.

**Table 1.** Data of the performed experiments.

Experiment No.	Average volumetric concentration, c%	Average flow velocity, U(m/s)	Pressure gradient DP/L, (kPa/m)
A1	2.91	1.16	0.86
A2	3.12	1.72	1.32
A3	3.00	1.95	1.62
A4	3.05	2.35	2.32
B1	4.86	1.75	1.63
B2	5.20	2.16	2.16
B3	4.93	2.35	2.52
C1	6.92	2.00	2.10
C2	6.88	2.32	2.62
D1	9.63	2.14	2.54
D2	10.03	2.32	2.97

Comparison of the velocity distribution for different average volumetric concentration is given in figure (11). The sequence of curves indicated that as the average concentration increased, the profile became more asymmetric due to increase of the concentration at the lower half of the tube which slowed the flow velocity there. This also was reflected on the values of  $(U_{max}/U)$  which increased and the position of the dynamic axis which became higher.

## CONCLUSION

Steady turbulent slurry flow in pipeline was studied both theoretically and experimentally. A simple formula was obtained to describe the velocity distribution as a function of the mixture properties, dynamic coefficient of turbulence, pressure gradient and concentration distribution across the pipe. Experimental measurements indicated that the proposed model provided accurate prediction of the velocity field for the range of volumetric concentration and average flow velocity used in the experiment.. The following concluding remarks may be drawn from the present work.

1. The main advantage of the model is its ability to reflect the particles, the fluid and the pipeline properties effects on the distribution of velocity using a simple algorithm that needs no complicated calculation.
2. Within the range of experiments, the model should predict the shape and the velocity distribution accurately with a maximum error of 7 %.





3. In the vertical mid-plane of the tube, the velocity profile is, in general, asymmetric with the dynamic axis above the geometric one.
4. Decreasing the volumetric concentration or increasing the mean flow velocity brings the flow closer to a homogeneous regime and the profile to a symmetric shape.
5. More development of the theoretical analysis should be carried out to include all the terms dropped in the present model to cover higher volumetric concentration range. Further experimental work is needed to evaluate these developments.

## ACKNOWLEDGEMENT

The authors express their appreciation for the help given by the fluid-mechanics technicians during the construction of the pipeline and to the staff of the Air Defence College, Alexandria for lending the gamma-ray equipment.

## REFERENCES

- [1] Durand R " Basic relationships of the transportation of solids in pipes-experimental research", Proc. Int. Assoc. Hydraulic Res. Minneapolis, 1-4 (1953).
- [2] Condiolos, E, and Chapus E.E. "Designing solid handling pipelines" Chemical Engng 70, 137 (1963).
- [3] Zandi I. and Govatos G., "Heterogeneous flow of solids in pipelines, J. The hydraulic Division ASCE, HY3, (1967).
- [4] Baird M.H.I, Round G.F. and Cardenas J.N., "Friction factors in pulsed turbulent flow". The Canadian J. of Ch. Engng, 49, 220 (1971).
- [5] Bagnold R.A " The flow of cohesionless grains in fluids", Phil. Trans. Royal Soc. Series A. 249, 964 (1956).
- [6] Wilson K.C., "Analytically-based nomographic charts for sand-water flow", Proc. Hydrotransport 4 paper A1. BHRA (1976).
- [7] Roco M.C. and Shook C.A., " Calculation model for turbulent slurry flow". Joint ASME-ASCE mech. conf., Colorado (1981).
- [8] Roco M.C. and Shook C.A. "New approach to predict concentration distribution in fine particle slurry flow" Physico Chemical Hydr. J. Vol 8-1, 43 (1987).
- [9] Yalin S.M. "Mechanics of sediment transport", Pergamon, Oxford (1972).
- [10] Wang S., "Variation of Karman Constant in Sediment Laden flow"; J. The Hydraulic Division, ASCE, HY4 (1981).
- [11] Shook C.A. and Daniel S.M., " A variable-density model for the pipeline flow of suspension. Can. J. of Chem Engng 47, 196 (1969).
- [12] Volcaldo J.J. and Charles M.E., "Prediction of the pressure gradient for the horizontal turbulent flow of slurries", Proc. Hydrotransport 2, BHRA Granfield (1972).
- [13] Wallis G.B. " One-dimensional Two-phase flow-McGraw Hill N.Y. (1969).
- [14] Peckenkin M.V., "Experimental Studies of Flows with high solid particle concentration", Proc 13th congress A.I.R.H., Tokyo (1972).
- [15] Roco M. C and Shook C.A., "Modeling of Slurry flow: the effect of particle size", Can. J. of Ch. Engng., Vol 61-4, 494, 1983.
- [16] Roco M. C and Frasincau "Computational method of two-phase liquid-solid flow indices



## 92 Computational Methods and Experimental Measurements

in pipelines and channel" *Stud. Cerc. Mecanica Aplicata*, 36 (3), (1977).

- [17] El Halawany M.A. " Velocity and concentration distribution of slurry flow in pipelines, M.Sc. thesis, Faculty of Engineering Alexandria University, Alexandria, Egypt (1988).
- [18] Kassab S.Z. Pitot tube as a calibration device for turbulence measurements, *Rev. Sci. Instrum*, 61 (6), 1757 (1990).
- [19] Yuan, S. W., "Foundations of fluid mechanics", Prentice Hall Inc., Englewood cliffs, New Jersey (1977).

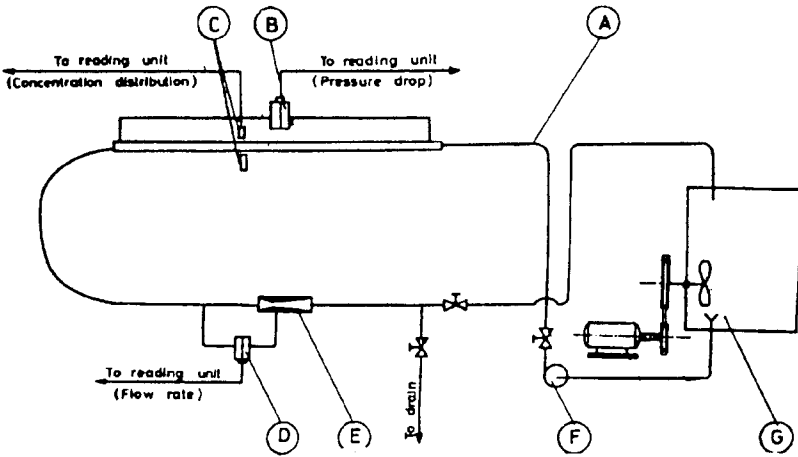


Figure 1. Schematic diagram of the experimental apparatus; A- Pipeline; B- Pressure transducer; c- Gamma-ray system; D- Pressure transducer; E- Venturi-meter; F- Pump; G- Mixing tank.

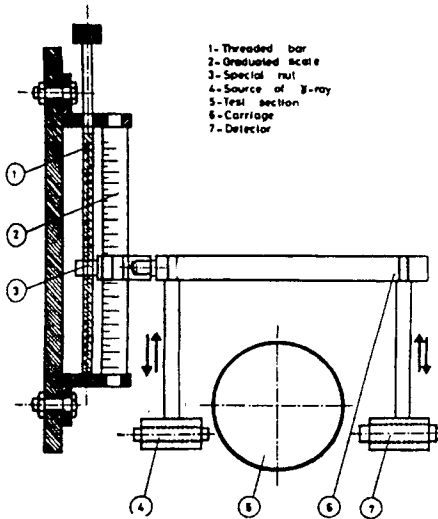


Figure 2. Traversing mechanism for the gamma-ray source and detector system.



## 94 Computational Methods and Experimental Measurements

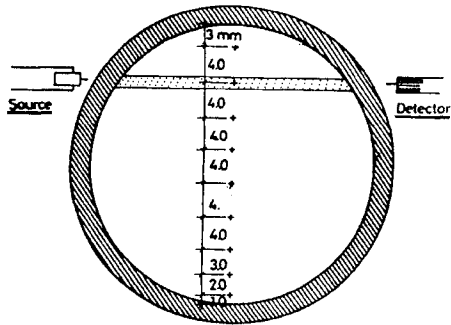


Figure 3. Measurement positions for concentration distribution.

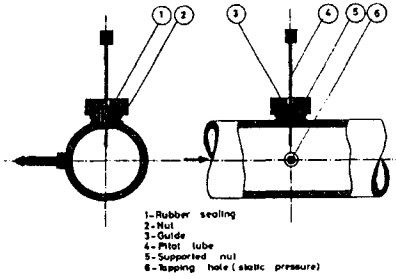


Figure 4. Measurements of velocity distribution using Pitot-system.

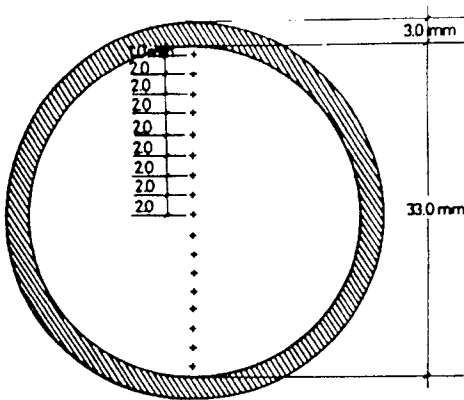


Figure 5. Measurement positions for velocity distribution.

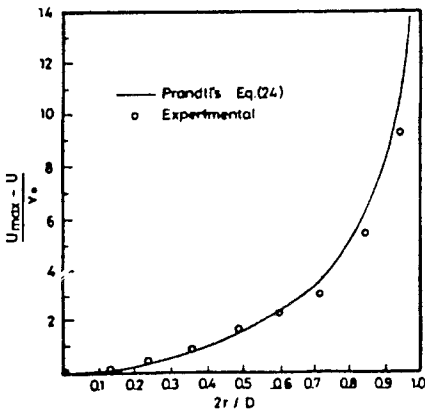


Figure 6. Calibration of the Pitot-system for fully developed turbulent flow of pure water.



## 96 Computational Methods and Experimental Measurements

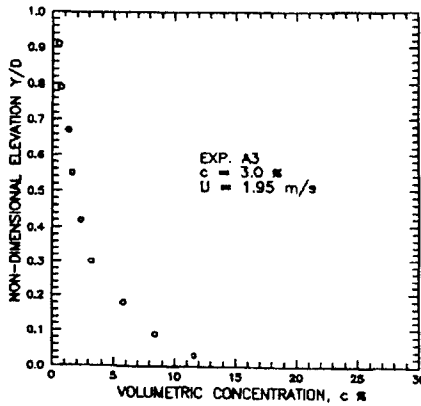
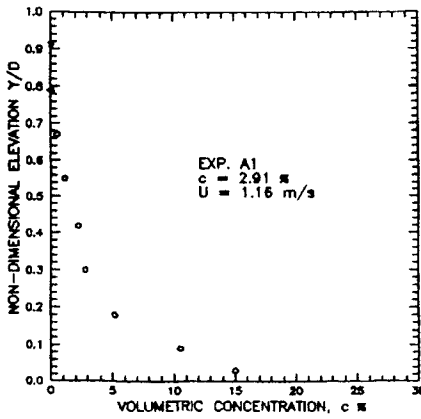


Figure 7. Concentration distribution for different flow rates (Approx. average concentration = 3 %).

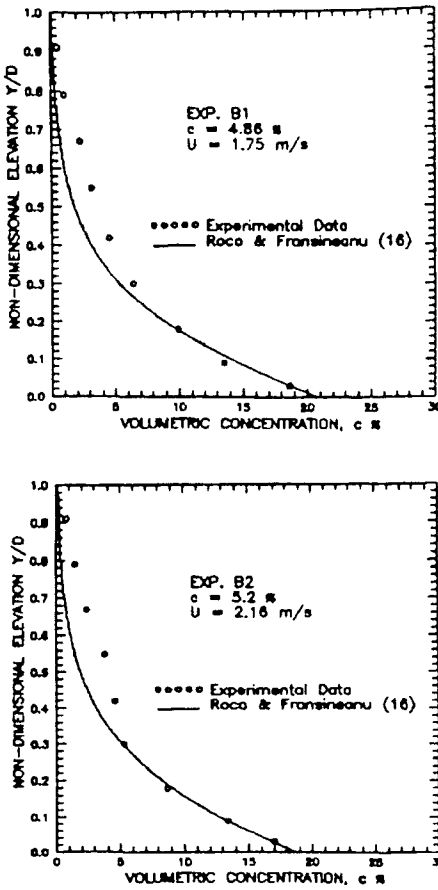


Figure 8. Concentration distribution for different flow rates (Approx. average concentration = 5 %).



## 98 Computational Methods and Experimental Measurements

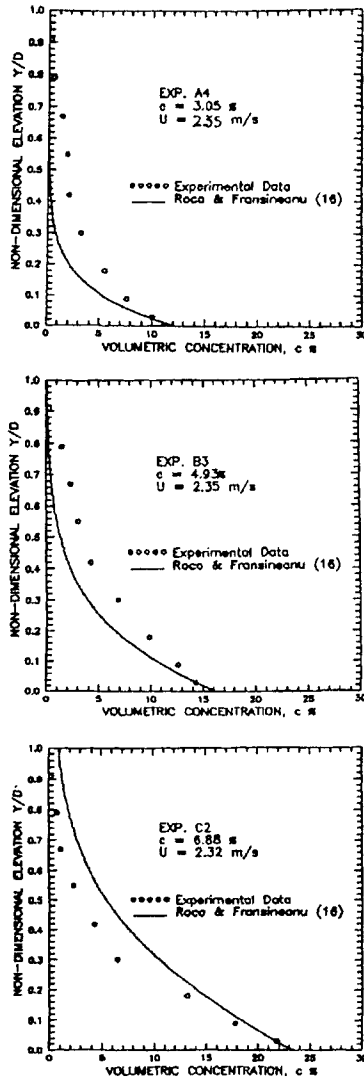
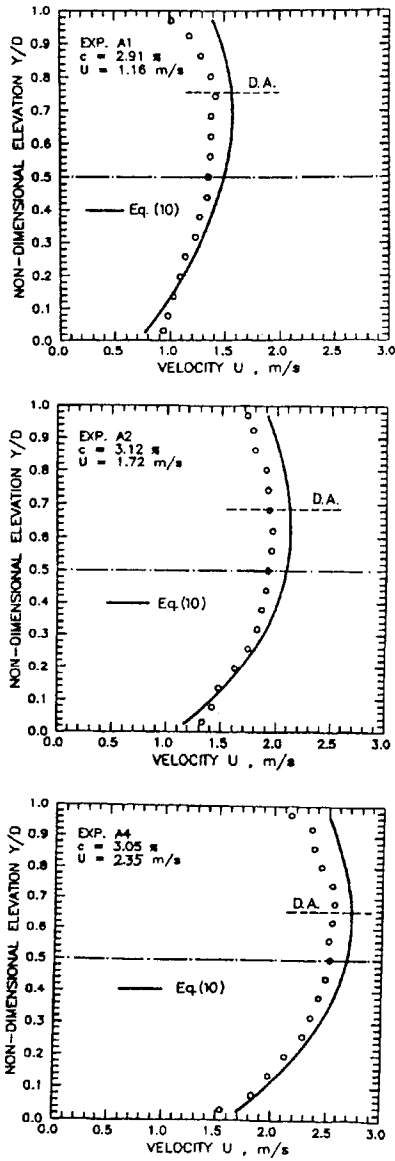


Figure 9. Comparison of Roco & Fransineanu model [16] with measurements of concentrationm distribution.





**Figure 10.** Velocity distribution for different flow rates (Approx. average concentration = 3 %).

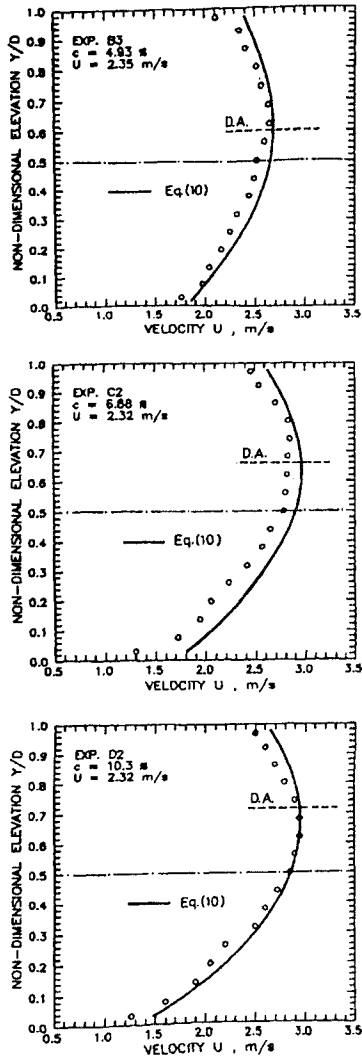


Figure 11. Velocity distribution for different average concentration (mean flow velocity 2.35 m/s).